

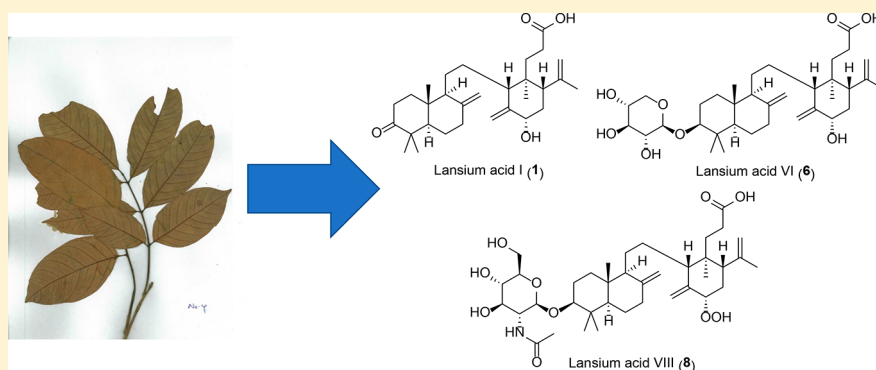
Structures and Antimutagenic Effects of Onoceranoid-Type Triterpenoids from the Leaves of *Lansium domesticum*

Takahiro Matsumoto,[†] Takahiro Kitagawa,[†] Stephen Teo,[‡] Yuuka Anai,[†] Risa Ikeda,[†] Daisuke Imahori,[†] Haji Sapuan bin Ahmad,[‡] and Tetsushi Watanabe^{*,†,§}

[†]Kyoto Pharmaceutical University, Misasagi, Yamashina-ku, Kyoto 607-8412, Japan

[‡]Forest Department Sarawak, Wisma Sumber Alam, Jalan Stadium, Petra Jaya, 93660 Kuching, Sarawak, Malaysia

Supporting Information



ABSTRACT: A methanol extract of the dried leaves of *Lansium domesticum* showed antimutagenic effects against 3-amino-1,4-dimethyl-5H-pyrido[4,3-b]indole (Trp-P-1) and 2-amino-1-methyl-6-phenylimidazo[4,5-b]pyridine (PhIP) using the Ames assay. Nine new onoceranoid-type triterpenoids, lansium acids I–IX (1–9), and nine known compounds (10–16) were isolated from the extract. The structures of the new compounds were elucidated on the basis of chemical and spectroscopic evidence. The absolute stereostructures of the new compounds were determined via their electronic circular dichroism spectra. Several isolated onoceranoid-type triterpenoids showed antimutagenic effects in an in vitro Ames assay. Moreover, oral intake of a major constituent, lansionic acid (10), showed antimutagenic effects against PhIP in an in vivo micronucleus test.

Lansium domesticum Corr. (Meliaceae), a fruit-bearing tree, grows widely in southeastern Asia.^{1–3} The fruits of this species are edible and are very popular in desserts. A number of onoceranoid-type triterpenoids have been reported from *L. domesticum* peels.^{4–6} Previous reports have described the bioactivities of these triterpenoids, such as toxicity against brine shrimp,¹ inhibition of leukotriene D4-induced contraction of guinea pig ileum,⁷ cytotoxic activity,⁸ and antibacterial activity against Gram-positive bacteria.⁹ As part of an ongoing research program for the discovery of new antimutagenic agents, our group has reported the structures and antimutagenic effects of *ent*-kaurane diterpenoids,¹⁰ coumarins,¹¹ and oximes.¹² As a continuation of these studies, we found that the MeOH extract of *L. domesticum* leaves showed antimutagenic effects against 3-amino-1,4-dimethyl-5H-pyrido[4,3-b]indole (Trp-P-1) [inhibition: 80.8% at 125 μ g/plate] and 2-amino-1-methyl-6-phenylimidazo[4,5-b]pyridine (PhIP) [inhibition: 75.7% at 125 μ g/plate], using the Ames test. According to these findings, the isolation of onoceranoid-type triterpenoids and the investigation of their antimutagenic effects were pursued. This paper reports the structure elucidation of lansium acids I–IX (1–9) and the antimutagenic activities of

the isolated onoceranoid-type triterpenoids (10–12, 16, and 17) using in vitro and in vivo bioassays.

RESULTS AND DISCUSSION

A methanol extract of *L. domesticum* dried leaves was partitioned with ethyl acetate–H₂O (1:1, v/v), to furnish an ethyl acetate-soluble fraction (2.1%) and an aqueous layer. The aqueous layer was further extracted with 1-butanol to give 1-butanol (1.3%) and H₂O (1.6%) soluble fractions. The ethyl acetate- and 1-butanol-soluble fractions were subjected to normal- and reversed-phase silica gel column chromatography and repeated high-performance liquid chromatography (HPLC) to give nine new compounds, lansium acids I (1, 0.0036%), II (2, 0.0042%), III (3, 0.012%), IV (4, 0.0025%), V (5, 0.00058%), VI (6, 0.00058%), VII (7, 0.0017%), VIII (8, 0.00073%), and IX (9, 0.00065%) together with nine known compounds, lansionic acid (10, 0.06%),⁷ methyl lansiolate (11, 0.002%),⁷ ethyl lansiolate (12, 0.0037%),⁹ lansioside C (13, 0.006%),⁷ lansioside B (14, 0.0013%),⁷ 8,14-*seco*-gammacer-7,14-diene-3,21-dione (15, 0.00047%),⁵ lansionic acid (16,

Received: April 30, 2018

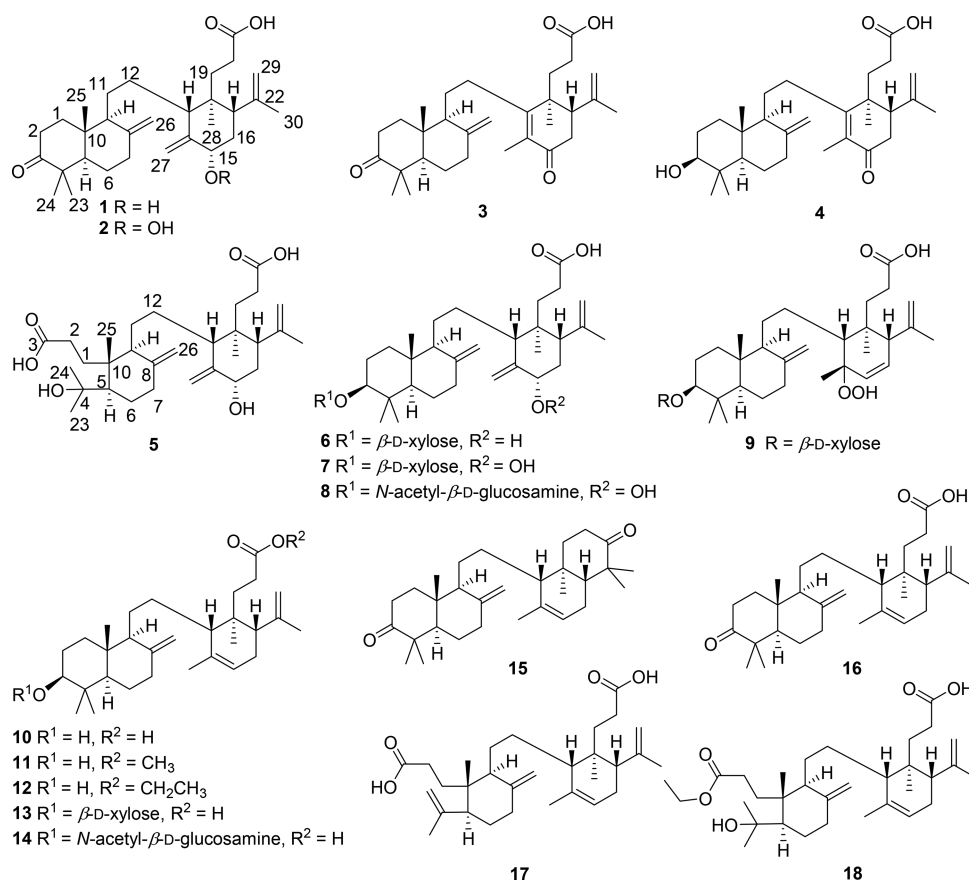


Figure 1. Chemical structures of isolated onoceranoid-type triterpenes from *Lansium domesticum*.

0.11%), ¹ lansic acid (17, 0.0088%), ¹ and lamesticum A (18, 0.00058%).⁹

Lansium acids I and II (1 and 2) were isolated as colorless, amorphous powders with positive optical rotations (1: $[\alpha]^{25}_D +11.1$, 2: $[\alpha]^{25}_D +11.3$ in methanol). Electrospray-ionization mass spectrometry (ESIMS) revealed for each a quasimolecular ion peak (1, m/z 493 $[M + Na]^+$, and 2, 509 $[M + Na]^+$), which, when combined with data from high-resolution mass spectrometry (HRESIMS) and ¹³C NMR, led to the molecular formulas for 1 ($C_{30}H_{46}O_4$) and 2 ($C_{30}H_{46}O_5$). The ¹H and ¹³C NMR ($CDCl_3$) spectra of 1 and 2 (Tables 1 and 2) showed characteristic signals of onoceranoid-type triterpenoids. They included five methyl groups [1: δ_H 0.67 (s, H-28), 0.82 (s, H-25), 1.01 (s, H-24), 1.09 (s, H-23), and 1.72 (s, H-30), 2: δ_H 0.63 (s, H-28), 0.83 (s, H-25), 1.02 (s, H-24), 1.09 (s, H-23), and 1.72 (s, H-30)], three exomethylene groups [1: δ_C 104.1 (C-27), 107.8 (C-26), 114.4 (C-29), 145.6 (C-22), 147.4 (C-8), and 149.5 (C-14), 2: δ_C 105.0 (C-27), 107.8 (C-26), 114.7 (C-29), 145.2 (C-14), 145.4 (C-22), and 147.4 (C-8)], a ketone carbonyl group [1: δ_C 217.2 (C-3), 2: δ_C 217.2 (C-3)], a carboxylic acid carbonyl [1: δ_C 177.7 (C-21), 2: δ_C 178.3 (C-21)], and a methine group bearing an oxygen function [1: δ_C 73.2 (C-15), 2: δ_C 86.2 (C-15)]. The above analysis suggested that lansium acids I and II (1 and 2) are onoceranoid-type triterpenoids.^{7–9}

The positions of the functional groups described above were determined based on COSY double-quantum filter (DQF COSY) and heteronuclear multiple bond correlation (HMBC) NMR spectroscopy, as shown Figure 2. Hence, long-range correlations were observed between the following proton and carbon pairs: H-9 and C-12; H-13 and C-12; H-23 and C-3, C-

4, and C-5; H-25 and C-1, C-5, C-9, and C-10; H-26 and C-7, C-8, and C-9; H-27 and C-13, C-14, and C-15; H-28 and C-13, C-17, C-18, and C-19; H-29 and C-17, C-22, and C-30; H-20 and C-21 (Figure 2). The relative configurations of 1 and 2 were determined via analysis of their nuclear Overhauser effect spectroscopy (NOESY) spectra (Figure 3). The NOESY cross-peaks of H-23/H-5, H-24/H-25, H-5/H-9, and H-25/H-11 indicated that the CH_2 -11, Me-24, and Me-25 moieties are on one side of each molecule and that H-5 is on the opposite side. The cross-peaks of H-13/H-15, H-15/H-16 β , H-16 α /H-30, H-28/H-30, and H-17/H-19 indicated that H-13, H-15, H-17, and CH_2 -19 are all on the same side. The suggested relative configurations of 1 and 2 were identical to reported onoceranoid-type triterpenes from *L. domesticum*.¹ Finally, the absolute configurations were elucidated as being identical to the known compound lansionic acid (16) via their electronic circular dichroism (ECD) spectra. ECD maxima of 1 [271.7 nm ($\Delta\epsilon$ +0.6), 317.6 nm ($\Delta\epsilon$ -0.6)] and 2 [274.6 nm ($\Delta\epsilon$ +0.6), 316.7 nm ($\Delta\epsilon$ -0.4)] were identical with those from the known compounds lansionic acid (16) [274.4 nm ($\Delta\epsilon$ +0.2), 318.2 nm ($\Delta\epsilon$ -0.2), observed in this study], lansionic acid methyl ester [275 nm ($\Delta\epsilon$ +0.06), 307 nm ($\Delta\epsilon$ -0.21), described in the literature],⁷ and onoceranedione I [289 nm ($\Delta\epsilon$ ca. +1.6), 302 nm ($\Delta\epsilon$ ca. -0.2), described in the literature].¹³ The absolute configurations of these known compounds have been established via X-ray analysis and chemical derivatization. On the basis of all this evidence, the chemical structures of lansium acids I and II (1 and 2) were characterized as shown in Figure 1.

Lansium acids III and IV (3 and 4) were isolated as colorless, amorphous powders with positive optical rotations

Table 1. ^{13}C NMR Data (150 MHz) of Lansium Acids I–IX (1–9) (δ in ppm)

position	1 ^a	2 ^a	3 ^a	4 ^a	5 ^b	6 ^b	7 ^b	8 ^b	9 ^b
1	37.6	37.6	37.5	36.9	34.4	37.5	37.3	37.1	37.5
2	34.7	34.7	34.6	27.8	30.3	27.7	27.8	27.4	27.9
3	217.2	217.2	216.6	78.5	178.6	88.7	88.8	89.2	89.0
4	47.8	47.8	47.8	39.1	74.7	40.2	40.2	39.8	40.2
5	55.2	55.3	55.1	54.6	53.0	55.2	55.2	55.1	55.3
6	25.1	25.1	25.1	23.6	29.2	24.4	24.6	24.6	24.7
7	37.8	37.8	37.8	38.1	38.8	38.9	38.9	38.9	39.0
8	147.4	147.4	147.1	147.9	152.1	152.6	149.6	149.6	149.0
9	56.4	56.3	57.9	58.7	51.4	57.7	57.6	58.3	58.9
10	39.3	39.3	39.7	39.8	43.1	39.8	39.8	39.8	40.0
11	22.3	22.2	23.9	24.0	21.3	22.7	22.6	22.7	25.0
12	22.5	22.3	30.5	30.6	22.3	23.0	23.3	23.5	25.1
13	47.9	47.9	163.0	163.5	43.9	43.9	44.6	44.9	44.0
14	149.5	145.2	133.2	133.1	150.0	150.0	148.1	148.1	85.0
15	73.2	86.2	198.3	198.4	73.7	73.4	86.6	86.7	133.6
16	39.1	34.2	39.0	39.0	38.0	38.3	33.9	33.9	132.3
17	48.4	48.4	46.9	47.0	44.1	44.2	44.6	44.6	49.8
18	41.1	41.4	42.1	42.1	42.4	42.4	42.2	42.2	42.3
19	31.8	31.7	33.7	33.7	34.0	33.9	33.8	33.7	34.5
20	27.4	27.5	29.3	29.3	28.7	29.4	29.2	29.3	29.6
21	177.7	178.3	178.2	178.5	176.8	176.8	176.6	176.6	176.6
22	145.6	145.4	145.1	145.2	148.1	148.1	147.4	147.4	147.0
23	26.0	25.9	26.0	28.3	35.3	28.5	28.6	17.1	28.7
24	21.6	21.6	21.6	15.4	28.3	17.1	17.1	28.5	17.2
25	14.0	14.0	14.1	14.5	19.6	15.1	15.1	15.0	15.1
26	107.8	107.8	107.5	106.7	107.2	107.4	107.3	107.3	107.5
27	104.1	105.0	12.2	12.2	109.1	108.5	112.2	112.2	21.9
28	17.7	17.6	21.3	21.3	17.5	17.6	17.5	17.5	20.6
29	114.4	114.7	115.8	115.7	114.3	114.3	114.6	114.6	116.5
30	23.1	23.1	22.6	22.5	24.4	24.6	24.2	24.2	24.0
1'						107.9	107.9	105.1	107.9
2'						75.9	75.9	57.9	75.9
3'						79.0	79.0	76.5	79.0
4'						71.6	71.6	72.9	71.6
5'						67.4	67.4	78.6	67.4
6'								63.3	
Ac								170.4	
								24.1	

^aMeasured in CDCl_3 . ^bMeasured in $\text{C}_5\text{D}_5\text{N}$.

(3: $[\alpha]^{25}_{\text{D}} +10.7$, 4: $[\alpha]^{25}_{\text{D}} +12.6$ in methanol). ESIMS revealed for each a quasimolecular ion peak (m/z 491 $[\text{M} + \text{Na}]^+$ for 3, 493 $[\text{M} + \text{Na}]^+$ for 4), from which the molecular formulas (3: $\text{C}_{30}\text{H}_{44}\text{O}_4$ and 4: $\text{C}_{30}\text{H}_{46}\text{O}_4$) were determined. The ^1H and ^{13}C NMR (CDCl_3) spectra of 3 (Tables 1 and 2) showed signals due to its onoceranoide-type triterpenoid structure, which were similar to 1. The main differences between 3 and 1 were the position of the double bond, the presence of one more carbonyl group [3: δ_{C} 198.3 (C-15)], and the absence of a hydroxy group. The positions of each group in 3 were determined based on DQF COSY and HMBC NMR spectroscopy, as shown in Figure 2. The ^1H and ^{13}C NMR (CDCl_3) spectra of 4 were very similar to those of 3 except for the absence of the carbonyl group at C-3 and the presence of one more hydroxy group [4: δ_{H} 3.27 (dd, $J = 4.1$, 12.4), δ_{C} 78.5 (C-3)]. From this information and the 2D NMR experiments, the planar structure of 4 was established. The relative and the absolute configurations of 3 and 4 were determined by analysis of their NOESY spectra (Figure 3) and with the ECD spectra 3 [256.1 nm ($\Delta\epsilon +0.9$), 316.7 nm ($\Delta\epsilon$

-0.6)] and 4 [252.7 nm ($\Delta\epsilon +0.7$), 317.2 nm ($\Delta\epsilon -0.4$)], similar to the determinations made for 1 and 2. Based on this evidence, the chemical structures of lansium acids III and IV (3 and 4) were characterized as shown in Figure 1.

Lansium acid V (5) was isolated as a colorless, amorphous powder with a positive optical rotation, $[\alpha]^{25}_{\text{D}} +4.4$, in methanol. ESIMS revealed a sodiated molecular ion peak at m/z 527 $[\text{M} + \text{Na}]^+$, from which the molecular formula, $\text{C}_{30}\text{H}_{48}\text{O}_6$, was determined, in conjunction with the HRESIMS and ^{13}C NMR data. The ^1H and ^{13}C NMR ($\text{C}_5\text{D}_5\text{N}$) spectra of 5 (Tables 1 and 2) showed signals for five methyl groups, three exomethylene groups, a methine bearing an oxygenated function, a quaternary carbon bearing an oxygenated function, and two carboxylic acid groups. The above analysis suggested that lansium acid V (5) is an oxidized analogue of lansic acid (17). Based on DQF COSY and HMBC spectroscopy, the positions of two hydroxy groups were elucidated as C-4 and C-15 (Figure 2). Specifically, long-range correlations were observed between the following proton and carbon pairs: H-23 and C-4, -5, H-24 and C-4, -5, and H-27 and C-13, -14, -15

Table 2. ^1H NMR Spectroscopic Data (600 MHz) of Lansium Acids I–V (1–5) (δ in ppm, J in Hz)

position	1 ^a	2 ^a	3 ^a	4 ^a	5 ^b
1	α 2.01 (m) β 1.44 (m)	α 2.00 (m) β 1.47 (m)	α 2.00 (m) β 1.57 (m)	α 1.74 (m) β 1.20 (m)	2.01 (μ)
2	α 2.37 (m) β 2.39 (m)	α 2.36 (dd, 3.4, 6.9) β 2.39 (m)	α 2.43 (m) β 2.57 (m)	α 1.57 (m) β 1.71 (m)	2.75 (m) 3.27 (m)
3				3.27 (dd, 4.1, 12.4)	
5	1.59 (m)	1.59 (m)	1.61 (dd, 2.8, 12.4)	1.09 (m)	1.92 (t-like, 11.7)
6	α 1.46 (m) β 1.68 (m)	α 1.50 (m) β 1.68 (m)	α 1.48 (dd, 4.1, 12.4) β 1.71 (m)	α 1.37 (m) β 1.77 (m)	α 1.41 (m) β 1.77 (m)
7	2.43 (m)	2.44 (m)	α 2.45 (m) β 2.00 (m)	α 2.42 (m) β 2.00 (m)	α 2.43 (t-like, 13.7) β 2.22 (m)
9	1.61 (m)	1.64 (m)	1.75 (m)	1.65 (m)	2.22 (d-like, 10.3)
11	1.23 (m)	1.23 (m)	1.56 (m)	1.74 (m)	1.76 (m)
12	1.64 (m)	1.70 (m)	1.99 (m) 2.41 (m)	2.09 (m)	1.77 (m)
13	1.68 (m)	1.70 (m)			3.03 (d-like, 11.0)
15	3.97 (dd, 4.8, 11.0)	4.28 (dd, 4.8, 11.6)			4.59 (br s)
16	α 1.61 (m) β 1.96 (m)	α 1.59 (m) β 2.02 (m)	α 2.45 (m) β 2.02 (m)	α 2.49 (dd, 8.9, 17.4) β 2.59 (dd, 8.9, 17.4)	1.97 (m)
17	2.29 (dd, 3.4, 13.0)	2.29 (dd, 3.4, 13.0)	2.64 (m)	2.64 (dd, 4.8, 8.9)	3.28 (m)
19	1.59 (d-like, 2.8, 12.0)	1.60 (dd-like, 5.5, 8.3)	1.83 (m)	1.84 (m)	2.01 (m)
20	1.76 (m) 2.12 (d-like, 2.8, 3.0) 2.39 (m)	1.74 (m) 2.13 (m) 2.39 (m)	1.91 (m) 2.13 (dt, 4.8, 11.7) 2.33 (dt, 4.8, 11.7)	1.93 (m) 2.02 (m) 2.35 (m)	2.72 (m) 2.86 (m)
23	1.09 (s)	1.09 (s)	1.01 (s)	1.00 (s)	1.37 (s)
24	1.01 (s)	1.02 (s)	1.02 (s)	0.77 (s)	1.33 (s)
25	0.82 (s)	0.83 (s)	0.85 (s)	0.67 (s)	0.90 (s)
26	4.66 (br s) 4.93 (br s)	4.66 (br s) 4.93 (br s)	4.66 (br s) 4.97 (br s)	4.59 (br s) 4.90 (br s)	4.78 (br s) 5.04 (br s)
27	4.80 (br s) 5.26 (br s)	4.83 (br s) 5.20 (br s)	1.80 (s)	1.81 (s)	4.86 (br s) 5.20 (br s)
28	0.67 (s)	0.63 (s)	1.14 (s)	1.13 (s)	0.76 (s)
29	4.70 (br s) 4.90 (br s)	4.70 (br s) 4.91 (br s)	4.76 (br s) 4.91 (br s)	4.76 (br s) 4.91 (br s)	4.84 (br s) 4.91 (br s)
30	1.72 (s)	1.72 (s)	1.67 (s)	1.67 (s)	1.76 (s)

^aMeasured in CDCl_3 . ^bMeasured in $\text{C}_5\text{D}_5\text{N}$.

(Figure 2). The relative configuration of **5** was determined via analysis of its NOESY spectrum (Figure 3). The absolute configuration was assumed to be the same as the other isolated onoceranoid-type triterpenes. On the basis of all the evidence obtained, the chemical structure of lansium acid V (**5**) was characterized as shown in Figure 1.

Lansium acids VI, VII, and VIII (**6**, **7**, and **8**) were isolated as colorless, amorphous powders with negative and positive optical rotations (**6**: $[\alpha]_{\text{D}}^{25} -17.4$, **7**: $[\alpha]_{\text{D}}^{25} -2.0$, **8**: $[\alpha]_{\text{D}}^{25} +7.5$ in MeOH). ESIMS revealed quasimolecular ion peaks (**6**: m/z 627 $[\text{M} + \text{Na}]^+$, **7**: m/z 643 $[\text{M} + \text{Na}]^+$, **8**: m/z 714 $[\text{M} +$

$\text{Na}]^+$) from which the molecular formulas (**6**: $\text{C}_{35}\text{H}_{56}\text{O}_8$, **7**: $\text{C}_{36}\text{H}_{56}\text{O}_9$, **8**: $\text{C}_{38}\text{H}_{61}\text{NO}_{10}$) were determined, in conjunction with HRESIMS and their ^{13}C NMR data. The ^1H and ^{13}C NMR ($\text{C}_5\text{D}_5\text{N}$) spectra suggested that lansium acids VI and VIII (**6** and **8**) are glycosides of lansium acid I (**1**) and that lansium acid VII (**7**) is a glycoside of lansium acid II (**2**). Acid hydrolysis of **6**, **7**, and **8** with 5% aqueous H_2SO_4 –1,4-dioxane yielded D-xylose (from **6** and **7**) and N-acetyl-D-glucosamine (from **8**), which were identified via HPLC of their chiral tolylthiocarbamoyl thiazolidine derivatives.^{14,15} The attachment of the glycosyl moiety to C-3 was identified by the HMBC cross-peak between the aglycone [**6**: δ_{C} 88.7 (C-3), **7**: δ_{C} 88.8 (C-3), **8**: δ_{C} 89.2 (C-3)] and glycosyl moieties [**6**: δ_{H} 4.71 (d, $J = 8.2$ Hz, H-1'), **7**: δ_{H} 4.69 (d, $J = 7.6$ Hz, H-1'), **8**: δ_{H} 4.93 (d, $J = 8.2$, H-1')]. The relative configurations of **6**, **7**, and **8** were determined via analysis of their NOESY spectra (Figure 3). Finally, the absolute configurations were elucidated from their ECD spectra [**6**: 268.2 nm ($\Delta\epsilon +0.8$), 315.8 nm ($\Delta\epsilon -0.8$); **7**: 273.1 nm ($\Delta\epsilon +0.1$), 317.6 nm ($\Delta\epsilon -0.04$); **8**: 275.1 nm ($\Delta\epsilon +0.4$), 317.1 nm ($\Delta\epsilon -0.2$)], similar to the procedure used for lansium acid I (**1**). On the basis of all the evidence obtained, the structures of lansium acids VI, VII, and VIII (**6**, **7**, and **8**) were characterized as shown in Figure 1.

Lansium acid IX (**9**) was isolated as a colorless, amorphous powder with a negative optical rotation, $[\alpha]_{\text{D}}^{25} -36.6$, in methanol. ESIMS revealed a quasimolecular ion peak m/z 643 $[\text{M} + \text{Na}]^+$, from which the molecular formula, $\text{C}_{35}\text{H}_{56}\text{O}_9$, was determined in conjunction with the HRESIMS and ^{13}C NMR data. The ^1H and ^{13}C NMR (CDCl_3) spectra of **9** (Tables 1 and 3) showed signals due to the presence of an onoceranoid-type triterpene glycoside, similar to the data from **7**. The main differences from **7** were the location of the double bond and the occurrence of a peroxy group. Thus, for **9**, the double bond was located at C-15,16 and the peroxy group located at C-14, as determined based on DQF COSY, and HMBC spectroscopy. Long-range correlations were observed between H-27 and C-13, C-14, and C-15. The relative and the absolute configurations of **9** were determined via analysis of their NOESY (Figure 3) and ECD spectra [257.2 nm ($\Delta\epsilon +0.2$), 317.6 nm ($\Delta\epsilon -0.2$)], similar to the procedure used to determine **1**. On the basis of all this evidence, the structure of lansium acid IX (**9**) was characterized as shown in Figure 1.

Antimutagenic activities of selected isolated onoceranoid-type triterpenes (**10**, **11**, **12**, **16**, and **17**) against Trp-P-1 and PhIP (Supporting Information, Tables S10 and S11) were evaluated using the Ames test with *S. typhimurium* TA98. The other isolated compounds were not tested, because of their limited amount available. Trp-P-1 and PhIP are well-known mutagenic and carcinogenic heterocyclic amines found in cooked meat. The test results obtained showed that these onoceranoid-type triterpenes possess antimutagenic effects against Trp-P-1 and PhIP without antimicrobial activity at the tested concentrations. Among the compounds tested, the antimutagenic effect of lansiolic acid (**10**) [inhibition: 73.8% at 100 nmol/plate] against Trp-P-1 was equivalent to that of the positive control nobiletin [inhibition: 56% at 80 nmol/plate]. Based on these results, interesting structure–activity relationships could be suggested. Specifically, lansiolic acid (**10**) with a carboxylic acid moiety showed more potent antimutagenic effects than its analogues with either a methyl ester moiety (**11**) [inhibition: 29.5% at 100 nmol/plate] or an ethyl ester moiety (**12**) [inhibition: 7.9% at 100 nmol/plate]. Among the esters, the ethyl ester compound showed weaker effects than

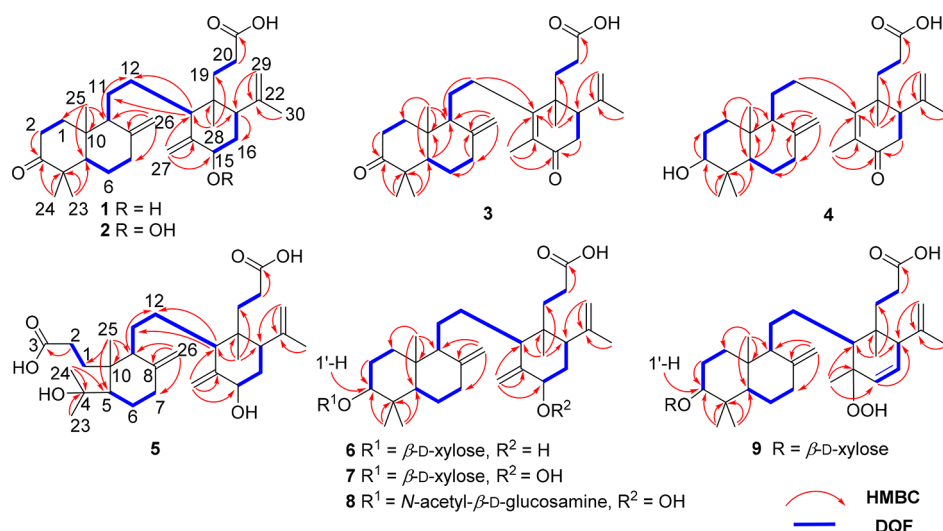


Figure 2. Important 2D NMR correlations in lansom acids I–IX (1–9).

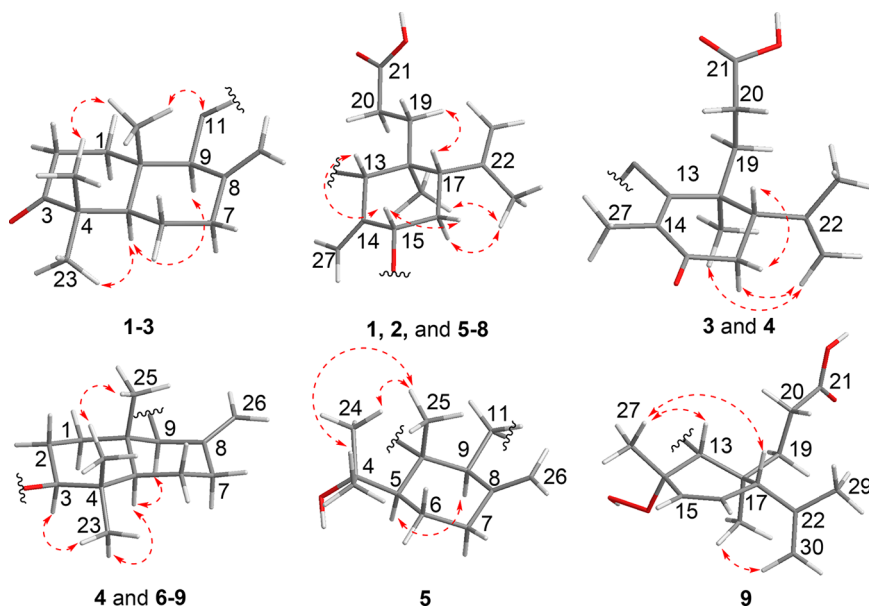


Figure 3. Important NOESY correlations of lansom acid I–IX (1–9).

the methyl ester. The effect of the compound with a hydroxy group at the C-3 position (10) was equivalent to the compound with a carbonyl group (16).

To examine the antimutagenic effects of major onoceranoide-type triterpenes of *L. domesticum* that showed positive effects in the Ames test, a micronucleus test was conducted using peripheral blood of male Institute of Cancer Research (ICR) mice. The micronucleus test is used to detect chromosomal damage induced by genotoxic compounds. It has been also used to evaluate the strength of antimutagenic agents in vivo.^{16–18} In this study, the in vivo antimutagenic effects of lansom acid (16) were evaluated against PhIP. Normal feed or sample feed that included lansom acid (16) was administrated at either a low or a high dose (0.03% or 0.06%, w/w). Mouse tail vein blood (5 μ L) was taken prior to administration of PhIP and 24, 48, and 72 h after test compound administration. Samples taken 24 and 48 h after lansom acid (16) administration showed that significantly

fewer micronucleated reticulocytes (MNRETs) were caused by PhIP (Figure 4).

EXPERIMENTAL SECTION

General Experimental Procedures. The following instruments were used to obtain physical data: specific rotations, a JASCO P-2200 digital polarimeter (l = 5 cm); JASCO FT/IR-4600 Fourier transform infrared spectrometer; ESIMS and high-resolution ESIMS, JEOL JMS-GCMATE mass spectrometer; ¹H NMR spectra, JEOL ECS400 (400 MHz) and JNM-ECA 600 K (600 MHz) spectrometers; ¹³C NMR spectra, JNM-ECA 600 K (150 MHz) spectrometer; 2D NMR spectra, JEOL JNM-ECA 600 K (600 MHz) spectrometer;

The following experimental materials were used for chromatography: normal-phase silica gel column chromatography, silica gel 60 (Kanto Chemical Co., Inc., 63–210 mesh); reversed-phase silica gel column chromatography, C₁₈-OPN (Nakalai Tesque Co., Inc. 140 μ m); thin-layer chromatography (TLC), precoated TLC plates with silica gel 60F₂₅₄ (Merck, 0.25 mm; ordinary phase) and silica gel RP-18 F_{254S} (Merck, 0.25 mm; reversed phase); reversed-phase high-performance TLC, precoated TLC plates with silica gel RP-18 WF_{254S} (Merck, 0.25 mm); HPLC, a Shimadzu SPD-M10Avp UV–vis

Table 3. ^1H NMR Data (600 MHz) of Lansium Acids VI–IX (6–9) (δ in ppm, J in Hz)^a

position	6	7	8	9
1	α 1.55 (m) β 1.22 (m)	α 1.58 (m) β 1.31 (m)	α 1.41 (m) β 1.16 (m)	α 1.90 (m) β 1.43 (m)
2	α 1.76 (m) β 1.98 (m)	α 1.74 (m) β 2.14 (m)	α 1.63 (m) β 2.17 (m)	α 1.79 (m) β 2.18 (m)
3	3.19 (dd, 4.1, 11.7)	3.23 (dd, 4.1, 11.7)	3.12 (dd, 1.8, 12.4)	3.30 (dd, 4.1, 11.7)
5	1.07 (d-like, 13.1)	1.09 (dd, 1.2, 12.4)	0.99 (dd, 2.0, 10.3)	1.11 (dd, 2.8, 13.1)
6	1.54 (m)	α 1.26 (m) β 1.60 (m)	1.27 (m)	α 1.26 (dd, 4.1, 13.1) β 1.60 (d-like, 13.1)
7	2.14 (m) 2.41 (m)	α 2.38 (d-like, 11.7) β 2.14 (dt, 1.2, 11.7)	α 2.40 (m) β 2.10 (m)	2.38 (d, 11.7)
9	1.83 (d-like, 10.3)	1.82 (m)	4.53 (m)	1.79 (d-like, 10.3)
11	1.46 (m)	1.49 (m)	1.41 (m)	1.43 (m)
12	1.60 (m) 1.85 (m)	1.81 (m)	1.52 (m)	1.79 (m)
13	3.00 (d-like, 11.7)	2.73 (d, 11.0)	2.75 (d, 11.0)	2.67 (d-like, 9.6)
15	4.62 (dr-s)	4.76 (m)	4.77 (br s)	5.91 (d, 10.4)
16	1.97 (m)	α 1.89 (dt, 2.8, 6.0) β 2.17 (m)	α 2.19 (m) β 1.91 (m)	5.70 (d-like, 10.4)
17	3.32 (dd, 6.2, 10.3)	2.98 (dd, 3.5, 17.2)	3.01 (d, 3.4, 9.6)	3.26 (br s)
19	1.98 (m)	1.98 (m)	2.03 (m)	2.04 (m)
20	2.71 (m) 2.95 (m)	2.61 (m) 2.80 (m)	2.60 (m) 2.81 (m)	2.69 (m) 2.79 (m)
23	1.19 (s)	1.18 (s)	0.90 (s)	1.21 (s)
24	0.91 (s)	0.89 (s)	1.06 (s)	0.90 (s)
25	0.61 (s)	0.59 (s)	0.53 (s)	0.61 (s)
26	4.74 (br s) 4.98 (br s)	4.77 (br s) 4.96 (br s)	4.75 (br s) 4.97 (br s)	4.95 (br s) 4.97 (br s)
27	4.84 (br s) 5.22 (br s)	5.03 (br s) 5.35 (br s)	5.05 (br s) 5.37 (br s)	1.42 (s)
28	0.78 (s)	0.72 (s)	0.74 (s)	1.82 (s)
29	4.88 (br s) 4.93 (br s)	4.76 (br s) 4.88 (br s)	4.79 (br s) 4.90 (br s)	4.85 (br s) 4.99 (br s)
30	1.78 (s)	1.69 (s)	1.71 (s)	1.75 (s)
1'	4.71 (d, 8.2)	4.69 (d, 7.6)	4.93 (d, 8.2)	4.72 (d, 8.2)
2'	3.69 (t, 8.2)	3.94 (t, 8.2)	1.75 (m)	3.94 (t, 8.2)
3'	4.13 (t, 8.2)	4.09 (t, 8.2)	4.36 (t, 10.3)	4.09 (t, 8.2)
4'	4.19 (m)	4.16 (m)	4.11 (t, 8.9)	4.14 (m)
5'	3.71 (t, 11.7) 4.29 (dd, 5.5, 11.6)	3.63 (t, 10.3) 4.21 (dd, 5.5, 10.3)	3.88 (m)	3.64 (t, 11.0) 4.21 (dd, 5.5, 11.0)
6'			4.29 (dd, 5.5, 11.7) 4.49 (d-like, 11.7) 2.10 (s)	
Ac				

^aMeasured in $\text{C}_5\text{D}_5\text{N}$.

detector. YMC Triart C₁₈ (250 × 4.6 mm i.d. and 250 × 10 mm i.d.) columns were used for analytical and preparative purposes.

Plant Material. The leaves of *Lansium domesticum* were collected in Ba'kelalan, Sarawak, Malaysia, in November 2015. The plant identification and the taxonomic authentication were conducted by one of the authors (S.T.). A voucher specimen (STTM-2015-4) has

been deposited in the Forest Herbarium, Forest Department Sarawak, Kuching, Sarawak, Malaysia.

Extraction and Isolation. Dried leaves of *L. domesticum* (550 g) were extracted three times with methanol under reflux for 3 h. Evaporation of the solvent provided a methanol extract (27.5 g, 5.0%). The methanol extract was partitioned into an ethyl acetate–water (1:1, v/v) mixture to furnish an ethyl acetate-soluble fraction (11.3 g, 2.1%) and an aqueous phase. The aqueous phase was further extracted with 1-butanol to give a 1-butanol-soluble fraction (7.2 g, 1.3%) and a water-soluble fraction (9.0 g, 1.6%). The ethyl acetate-soluble fraction was subjected to normal-phase silica gel column chromatography [250 g, *n*-hexane– CHCl_3 (3:1 → 2:1 → 1:1 → 1:2 → 0:1, v/v) → CHCl_3 –MeOH (100:1 → 50:1 → 30:1 → 10:1, v/v)], to give 10 fractions. Fraction EA5 (0.69 g) was further separated via reversed-phase silica gel column chromatography, to give eight fractions. Fraction EA5-4 (100.2 mg) was purified via HPLC [H_2O – CH_3CN – CH_3COOH (20:80:0.1, v/v/v)] to give **15** (2.6 mg). Fraction EA6 (1.50 g) was separated via reversed-phase silica gel column chromatography to give 10 fractions. Fraction EA6-6 (31.1 mg) was purified via HPLC [H_2O – CH_3CN – CH_3COOH (25:75:0.1, v/v/v)] to give **1** (20.0 mg) and **2** (23.0 mg). Fraction EA6-9 (903.3 mg) was purified via HPLC [H_2O – CH_3CN – CH_3COOH (5:95:0.1, v/v/v)] to give **16** (603.6 mg). Fraction EA8 (3.11 g) was separated by reversed-phase silica gel column chromatography to give 12 fractions. Fraction EA8-9 (616.0 mg) was purified via HPLC [H_2O – CH_3CN – CH_3COOH (10:90:0.1, v/v/v)] to give **10** (328.3 mg) and **18** (3.2 mg). Fraction EA8-10 (383.6 mg) was purified via HPLC [H_2O – CH_3CN – CH_3COOH (2:98:0.1, v/v/v)] to give **11** (11.2 mg) and **12** (20.1 mg).

The BuOH-soluble fraction was subjected to normal-phase silica gel column chromatography, [150 g, CHCl_3 –MeOH (100:1 → 50:1 → 20:1 → 10:1 → 5:1 → 2:1 → 1:1, v/v)], to give nine fractions. Fraction B3 (1.0 g) was further separated via reversed-phase silica gel column chromatography, to give eight fractions. Fraction B3-4 (218.8 mg) was purified via HPLC [H_2O – CH_3CN – CH_3COOH (40:60:0.1, v/v/v)] to give **3** (65.3 mg) and **4** (14.0 mg). Fraction B3-6 (147.1 mg) was purified via HPLC [H_2O – CH_3CN – CH_3COOH (10:90:0.1, v/v/v)] to give **17** (48.4 mg). Fraction B5 (1.0 g) was further separated via reversed-phase silica gel column chromatography to give nine fractions. Fraction B5-4 (184.6 mg) was purified via HPLC [H_2O – CH_3CN – CH_3COOH (40:60:0.1, v/v/v)] to give **6** (5.0 mg), **7** (9.3 mg), and **9** (3.6 mg). Fraction B5-5 (129.4 mg) was purified via HPLC [H_2O – CH_3CN – CH_3COOH (20:80:0.1, v/v/v)] to give **13** (32.8 mg). Fraction B7 (0.9 g) was further separated via reversed-phase silica gel column chromatography, to give nine fractions. Fraction B7-3 (126.7 mg) was purified via HPLC [H_2O – CH_3CN – CH_3COOH (60:40:0.1, v/v/v)] to give **5** (3.2 mg). Fraction B7-4 (112.4 mg) was purified via HPLC [H_2O – CH_3CN – CH_3COOH (60:40:0.1, v/v/v)] to give **8** (4.0 mg). Fraction B7-5 (55.6 mg) was purified via HPLC [H_2O – CH_3CN – CH_3COOH (60:40:0.1, v/v/v)] to give **14** (7.2 mg).

Lansium acid I (1): colorless, amorphous powder; [α]_D²⁵ +11.3 (c 0.35, MeOH); ECD (MeOH) [271.7 nm ($\Delta\epsilon$ +0.6), 317.6 nm ($\Delta\epsilon$ −0.6)]; IR (ATR) ν_{max} 2942, 1749, 1705, 1451, 1378, 1218, 1032 cm^{-1} ; ^1H (CDCl_3 , 600 MHz) and ^{13}C NMR (CDCl_3 , 150 MHz), see [Tables 1](#) and [2](#); ESIMS m/z 493 [$\text{M} + \text{Na}$]⁺; HRESIMS m/z 493.3290 [$\text{M} + \text{Na}$]⁺ (calcd for $\text{C}_{30}\text{H}_{46}\text{O}_4$, 493.3288).

Lansium acid II (2): colorless, amorphous powder; [α]_D²⁵ +11.1 (c 0.14, MeOH); ECD (MeOH) [274.6 nm ($\Delta\epsilon$ +0.6), 316.7 nm ($\Delta\epsilon$ −0.4)]; IR (ATR) ν_{max} 2931, 2854, 1701, 1455, 1400, 1377, 1243, 1218, 1065 cm^{-1} ; ^1H (CDCl_3 , 600 MHz) and ^{13}C NMR (CDCl_3 , 150 MHz), see [Tables 1](#) and [2](#); ESIMS m/z 509 [$\text{M} + \text{Na}$]⁺; HRESIMS m/z 509.3232 [$\text{M} + \text{Na}$]⁺ (calcd for $\text{C}_{30}\text{H}_{46}\text{O}_5$, 509.3237).

Lansium acid III (3): colorless, amorphous powder; [α]_D²⁵ +10.7 (c 0.47, MeOH); ECD (MeOH) [256.1 nm ($\Delta\epsilon$ +0.9), 316.7 nm ($\Delta\epsilon$ −0.6)]; IR (ATR) ν_{max} 2931, 2836, 1705, 1447, 1381 cm^{-1} ; ^1H (CDCl_3 , 600 MHz) and ^{13}C NMR (CDCl_3 , 150 MHz), see [Tables 1](#) and [2](#); ESIMS m/z 491 [$\text{M} + \text{Na}$]⁺; HRESIMS m/z 491.3134 (calcd for $\text{C}_{30}\text{H}_{44}\text{O}_4$ [$\text{M} + \text{Na}$]⁺, 491.3132).

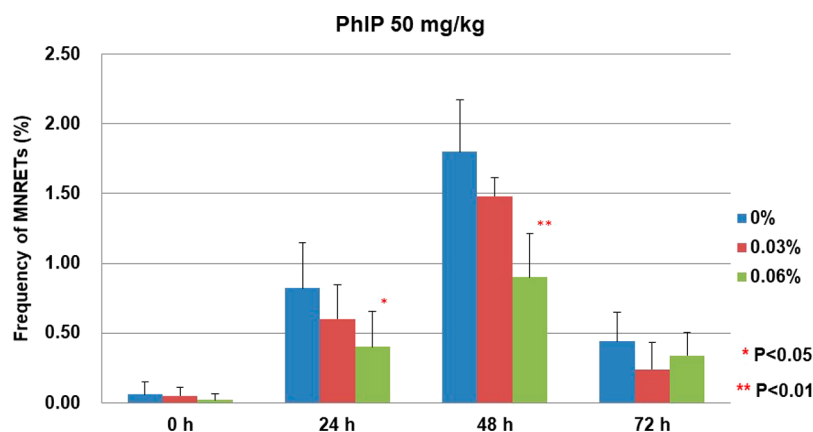


Figure 4. Frequency of micronucleated reticulocytes (MNRETs) from the peripheral blood of mice treated with a mutagen [PhIP (50 mg/kg body weight)]. Normal feed or sample feed that included lansonic acid (**16**) at a low or a high dose (0.03% or 0.06%, w/w) was given ad libitum. Significant difference: * $0.01 < p < 0.05$; ** $p < 0.01$ (Student's t test).

Lansium acid IV (4): colorless, amorphous powder; $[\alpha]_D^{25} +12.6$ (c 0.38, MeOH); ECD (MeOH) [252.7 nm ($\Delta\epsilon$ +0.7), 317.2 nm ($\Delta\epsilon$ -0.4)]; IR (ATR) ν_{\max} 2931, 2872, 1705, 1455, 1414, 1262 cm^{-1} ; ^1H ($\text{C}_5\text{D}_5\text{N}$, 600 MHz) and ^{13}C NMR ($\text{C}_5\text{D}_5\text{N}$, 150 MHz), see Tables 1 and 2; ESIMS m/z 493 $[\text{M} + \text{Na}]^+$; HRESIMS m/z 493.3291 $[\text{M} + \text{Na}]^+$ (calcd for $\text{C}_{30}\text{H}_{46}\text{O}_4$, 493.3288).

Lansium acid V (5): colorless, amorphous powder; $[\alpha]_D^{25} +4.4$ (c 0.16, MeOH); IR (ATR) ν_{\max} 2931, 2887, 1705, 1644, 1385, 1283, 1192, 1123 cm^{-1} ; ^1H ($\text{C}_5\text{D}_5\text{N}$, 600 MHz) and ^{13}C NMR ($\text{C}_5\text{D}_5\text{N}$, 150 MHz), see Tables 1 and 2; ESIMS m/z 527 $[\text{M} + \text{Na}]^+$; HRESIMS m/z 527.3349 $[\text{M} + \text{Na}]^+$ (calcd for $\text{C}_{30}\text{H}_{48}\text{O}_6$, 527.3343).

Lansium acid VI (6): colorless, amorphous powder; $[\alpha]_D^{25} -17.4$ (c 0.25, MeOH); ECD (MeOH) [268.2 nm ($\Delta\epsilon$ +0.8), 315.8 nm ($\Delta\epsilon$ -0.8)]; IR (ATR) ν_{\max} 2927, 2884, 1705, 1644, 1200, 1163 cm^{-1} ; ^1H ($\text{C}_5\text{D}_5\text{N}$, 600 MHz) and ^{13}C NMR ($\text{C}_5\text{D}_5\text{N}$, 150 MHz), see Tables 1 and 3; ESIMS m/z 627 $[\text{M} + \text{Na}]^+$; HRESIMS m/z 627.3863 $[\text{M} + \text{Na}]^+$ (calcd for $\text{C}_{35}\text{H}_{56}\text{O}_8$, 627.3867).

Lansium acid VII (7): colorless, amorphous powder; $[\alpha]_D^{25} -2.0$ (c 0.47, MeOH); ECD (MeOH) [273.1 nm ($\Delta\epsilon$ +0.1), 317.6 nm ($\Delta\epsilon$ -0.04)]; IR (ATR) ν_{\max} 2931, 2886, 1705, 1644, 1381, 1262, 1090 cm^{-1} ; ^1H ($\text{C}_5\text{D}_5\text{N}$, 600 MHz) and ^{13}C NMR ($\text{C}_5\text{D}_5\text{N}$, 150 MHz), see Tables 1 and 3; ESIMS m/z 643 $[\text{M} + \text{Na}]^+$; HRESIMS m/z 643.3819 $[\text{M} + \text{Na}]^+$ (calcd for $\text{C}_{35}\text{H}_{56}\text{O}_9$, 643.3817).

Lansium acid VIII (8): colorless, amorphous powder; $[\alpha]_D^{25} +7.5$ (c 0.2, MeOH); ECD (MeOH) [275.1 nm ($\Delta\epsilon$ +0.4), 317.1 nm ($\Delta\epsilon$ -0.2)]; IR (ATR) ν_{\max} 2890, 2836, 1708, 1640, 1385, 1112 cm^{-1} ; ^1H ($\text{C}_5\text{D}_5\text{N}$, 600 MHz) and ^{13}C NMR ($\text{C}_5\text{D}_5\text{N}$, 150 MHz), see Tables 1 and 3; ESIMS m/z 714 $[\text{M} + \text{Na}]^+$; HRESIMS m/z 714.4182 $[\text{M} + \text{Na}]^+$ (calcd for $\text{C}_{38}\text{H}_{61}\text{NO}_{10}$, 714.4188).

Lansium acid IX (9): colorless, amorphous powder; $[\alpha]_D^{25} -36.6$ (c 0.18, MeOH); ECD (MeOH) [257.2 nm ($\Delta\epsilon$ +0.2), 317.6 nm ($\Delta\epsilon$ -0.2)]; IR (ATR) ν_{\max} 2927, 2886, 1708, 1640, 1380, 1163 cm^{-1} ; ^1H ($\text{C}_5\text{D}_5\text{N}$, 600 MHz) and ^{13}C NMR ($\text{C}_5\text{D}_5\text{N}$, 150 MHz), see Tables 1 and 3; ESIMS m/z 643 $[\text{M} + \text{Na}]^+$; HRESIMS m/z 643.3815 $[\text{M} + \text{Na}]^+$ (calcd for $\text{C}_{35}\text{H}_{56}\text{O}_9$, 643.3817).

Acid Hydrolysis and Monosaccharide Identification of Compounds 6–9. Identification of the monosaccharides of 6–9 was performed according to the method reported by Tanaka et al. with slight modifications.¹⁴ After the acid hydrolysis of 6–9, chiral tolylthiocarbamoyl thiazolidine derivatives were obtained. Each solution was analyzed via HPLC [column: Cosmosil SC18-AR-II (Nacalai Tesque), 250 \times 4.6 mm i.d. (5 μm); mobile phase: 25% CH_3CN in 50 mM H_3PO_4 ; detection: UV (254 nm); flow rate: 0.8 mL/min; column temperature: 25 $^\circ\text{C}$] to identify the derivatives of the constituents D-xylose (6, 7, and 9) and N-acetyl-D-glucosamine (8) by comparison of their retention times with those of authentic samples (t_R : D-xylose, 16.37 min, N-acetyl-D-glucosamine, 35.29 min).

Evaluation of in Vitro Antimutagenic Activity Using the Ames Test. Antimutagenicity was examined via the preincubation

method using *Salmonella typhimurium* TA98 with S9 mix, as described previously.^{10,12} PhIP (1 μg) and Trp-P-1 (0.04 μg) were used as mutagens to examine the antimutagenic activity of the samples. The experiments were conducted according to the Guidelines for Animal Experiments at Kyoto Pharmaceutical University (KPU), and the animal studies were approved by the Experimental Animal Research Committee (permission number: 17-030).

Evaluation of in Vivo Antimutagenic Effects using Micronucleus Test. The in vivo micronucleus test was carried out according to a method published previously.^{11,19} Briefly, for the test group, sample feed [lansonic acid (**16**)-containing feed] was ingested 2 days before and throughout the experiment. Feed containing 0.03–0.06% w/w lansonic acid (**16**) was prepared by thoroughly mixing lansonic acid (**16**) with CE-2 powder diet (Clea Japan, Inc., Tokyo, Japan). PhIP (50 mg/kg bodyweight) was administered intraperitoneally to mice in all groups to induce micronuclei. Mouse tail vein blood (5 μL) was taken prior to the administration of PhIP and 24, 48, and 72 h after the administration of the test samples. Observations were made using an excitation filter, and an absorbing filter (Nikon fluorescence block B-2A, Nikon, Ltd.) epi-equipped with a fluorescence microscope [power supply HB-10101AF, OPTIPHOT-2 lens (400 times), Nikon, Ltd.] was used. One thousand reticulocytes were observed per slide, and those including micronuclei were counted. Statistics regarding micronucleus frequency were calculated using Student's t test. Significance levels were set at 5% and 1%. The animal studies were approved by the Experimental Animal Research Committee at KPU (permission number: 17-031).

■ ASSOCIATED CONTENT

● Supporting Information

The Supporting Information is available free of charge on the ACS Publications website at DOI: 10.1021/acs.jnatprod.8b00341.

Experimental details, including ESIMS, HRESIMS, ^1H and ^{13}C NMR spectra, 2D NMR spectra, and the results of the Ames assay (PDF)

■ AUTHOR INFORMATION

Corresponding Author

*Tel: +81-75-595-4650. Fax: +81-75-595-4769. E-mail: watanabe@mb.kyoto-phu.ac.jp.

ORCID

Tetsushi Watanabe: 0000-0002-5190-9244

Notes

The authors declare no competing financial interest.

■ ACKNOWLEDGMENTS

This work was supported by JSPS KAKENHI Grant Number JP17K15473.

■ REFERENCES

- (1) Tanaka, T.; Ishibashi, M.; Fujimoto, H.; Okuyama, E.; Koyano, T.; Kowithayakorn, T.; Hayashi, M.; Komiyama, K. *J. Nat. Prod.* **2002**, *65*, 1709–1711.
- (2) Kiang, A. K.; Tan, E. L.; Lim, F. Y.; Habaguchi, K.; Nakanishi, K.; Fachan, L.; Ourisson, G. *Tetrahedron Lett.* **1967**, *8*, 3571–3574.
- (3) Rudiyanisya; Alimuddin, A. H.; Masriani; Muharini, R.; Proksch, P. *Phytochem. Lett.* **2018**, *23*, 90–93.
- (4) Saewan, N.; Sutherland, J. D.; Chantrapromma, K. *Phytochemistry* **2006**, *67*, 2288–2293.
- (5) Habaguchi, K.; Watanabe, M.; Nakadaira, Y.; Nakanishi, K. *Tetrahedron Lett.* **1968**, *34*, 3731–3734.
- (6) Mayanti, T.; Tjokronegoro, R.; Supratman, U.; Mukhtar, M. R.; Awang, K.; Hadi, A. H. *Molecules* **2011**, *16*, 2785–2795.
- (7) Nishizawa, M.; Nishida, H.; Kosela, S.; Hayashi, Y. *J. Org. Chem.* **1983**, *48*, 4462–4466.
- (8) Nugroho, A. E.; Inoue, D.; Wong, C. P.; Hirasawa, Y.; Kaneda, T.; Shiota, O.; Hadi, A. H.; Morita, H. *J. Nat. Med.* **2018**, *72*, 588–592.
- (9) Dong, S. H.; Zhang, C. R.; Dong, L.; Wu, Y.; Yue, J. M. *J. Nat. Prod.* **2011**, *74*, 1042–1048.
- (10) Matsumoto, T.; Nakamura, S.; Kojima, N.; Hasei, T.; Yamashita, M.; Watanabe, T.; Matsuda, H. *Tetrahedron Lett.* **2017**, *58*, 3574–3578.
- (11) Matsumoto, T.; Takahashi, K.; Kanayama, S.; Nakano, Y.; Imai, H.; Kibi, M.; Imahori, D.; Hasei, T.; Watanabe, T. *J. Nat. Med.* **2017**, *71*, 735–744.
- (12) Matsumoto, T.; Koike, M.; Arai, C.; Kitagawa, T.; Inoue, E.; Imahori, D.; Watanabe, T. *Phytochem. Lett.* **2018**, *25*, 118–121.
- (13) Tsuda, Y.; Yamashita, T.; Sano, T. *Chem. Pharm. Bull.* **1984**, *32*, 4820–4832.
- (14) Tanaka, T.; Nakashima, T.; Ueda, T.; Tomii, K.; Kouno, I. *Chem. Pharm. Bull.* **2007**, *55*, 899–901.
- (15) Nakamura, S.; Fujimoto, K.; Matsumoto, T.; Nakashima, S.; Ohta, T.; Ogawa, K.; Matsuda, H.; Yoshikawa, M. *Phytochemistry* **2013**, *92*, 128–136.
- (16) Lima, D. C.; Vale, C. R.; Veras, J. H.; Bernardes, A.; Perez, C. N.; Chen-Chen, L. *PLoS One* **2017**, *16*, e0171224.
- (17) Di Giorgio, C.; Boyer, L.; De Meo, M.; Laurant, C.; Elias, R.; Ollivier, E. *J. Nat. Med.* **2015**, *69*, 267–277.
- (18) Rodrigues, C. R.; Dias, J. H.; de Mello, R. N.; Richter, M. F.; Picada, J. N.; Ferraz, A. B. *J. Ethnopharmacol.* **2009**, *17*, 97–101.
- (19) Matsumoto, T.; Nishikawa, T.; Furukawa, A.; Itano, S.; Tamura, Y.; Hasei, T.; Watanabe, T. *Nat. Prod. Commun.* **2017**, *12*, 23–26.